The nature of dissipation in compressible MHD turbulence

Thibaud RICHARD, Pierre LESAFFRE

Thanks : Edith FALGARONE, Andrew LEHMANN

Numerical method – Simulations

- **Isothermal compressible MHD simulations (1024^3 cells) using a modified version of the RAMSES code (CHEMSES by Lesaffre et al, 2020):**

Mass conservation :	$\partial_t \rho + \vec{\nabla} \cdot (\rho \vec{u}) = 0$
Momentum conservation :	$\rho(\partial_t \vec{u} + (\vec{u} \cdot \nabla)\vec{u}) = -\vec{\nabla} p + \vec{J} \times \vec{B} + \mu \nabla^2 \vec{u} + \frac{\mu}{3} \vec{\nabla} \left(\vec{\nabla} \cdot \vec{u} \right)$
Induction :	$\partial_t \vec{B} = \nabla \times (\vec{u} \times \vec{B}) + \eta \nabla^2 \vec{B}$

Decaying turbulence, starting at equipartion $\langle \rho u^2 \rangle \simeq \langle \frac{B^2}{4\pi} \rangle$

Initial conditions of our fiducial simulations:

Arnold Beltrami Childress
ABC (has magnetic helicity)

Orszag-Tang
OT (has cross helicity)

$\mathcal{M}_{\rm s} = 4$ $\quad \mathcal{M}_{\rm A} = 1$

$R_e \simeq 10^4$ $\quad R_{e_m} \simeq 10^4$

In the diffuse phase : $R_e \simeq 2.10^7$ $\quad R_{e_m} \simeq 2.10^{17}$

Numerical method - Dissipation in simulations

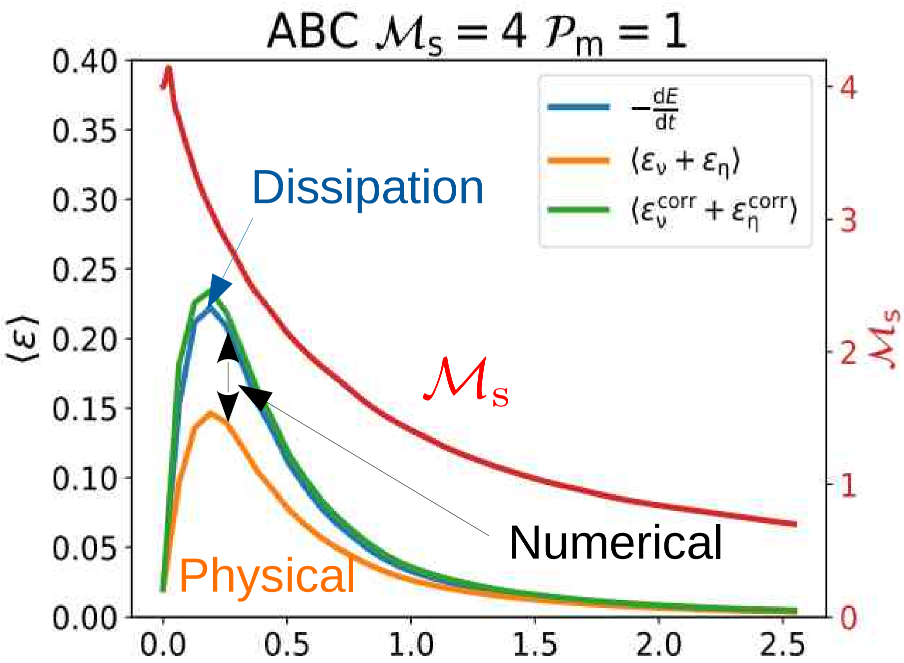

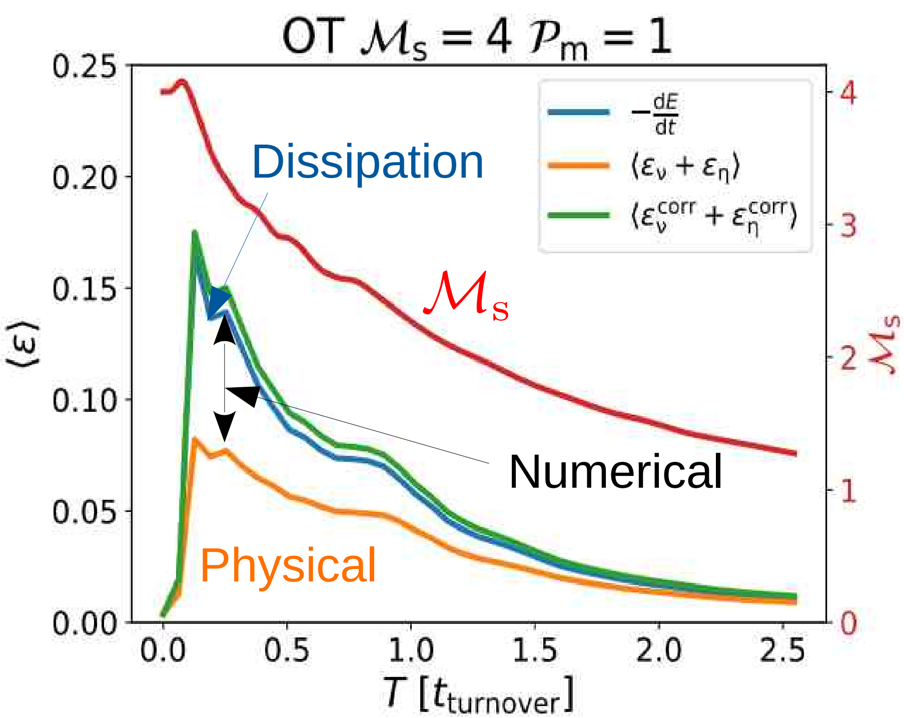

The overall budget of the generalized mechanical energy dissipated:

$$\frac{\mathrm{dE}}{\mathrm{dt}} = \frac{\mathrm{d}}{\mathrm{dt}}\langle \frac{1}{2}\rho u^2 + \frac{1}{8\pi}B^2 + p\log\rho \rangle$$

Calculated irreversible dissipation rate (Physical):

$$\varepsilon = \varepsilon_\nu + \varepsilon_\eta = \sigma_{ij}\partial_i u_j + \eta J^2$$

Viscous Ohmic

$$\sigma_{ij} = \mu(\partial_i u_j + \partial_j u_i - \frac{2}{3}\partial_k u_k \delta_{ij})$$

Estimated real irreversible dissipation rate (Physical +numérical):

$$\partial_t(\frac{1}{2}\rho u^2 + \frac{1}{8\pi}B^2 + p\log\rho) + \vec{\nabla}\cdot\vec{\mathcal{F}}_2 = -\varepsilon_{\mathrm{tot}}$$

➡ We recover the local numerical dissipation that is not taken into account by the physical determination of dissipation.

Numerical methods - Structure extraction

ABC, initial sonic Mach number = 4, near the dissipation peak:

The first contour is at : $\varepsilon_{\mathrm{tot}} = \langle \varepsilon_{\mathrm{tot}} \rangle + 4 \times \sigma$

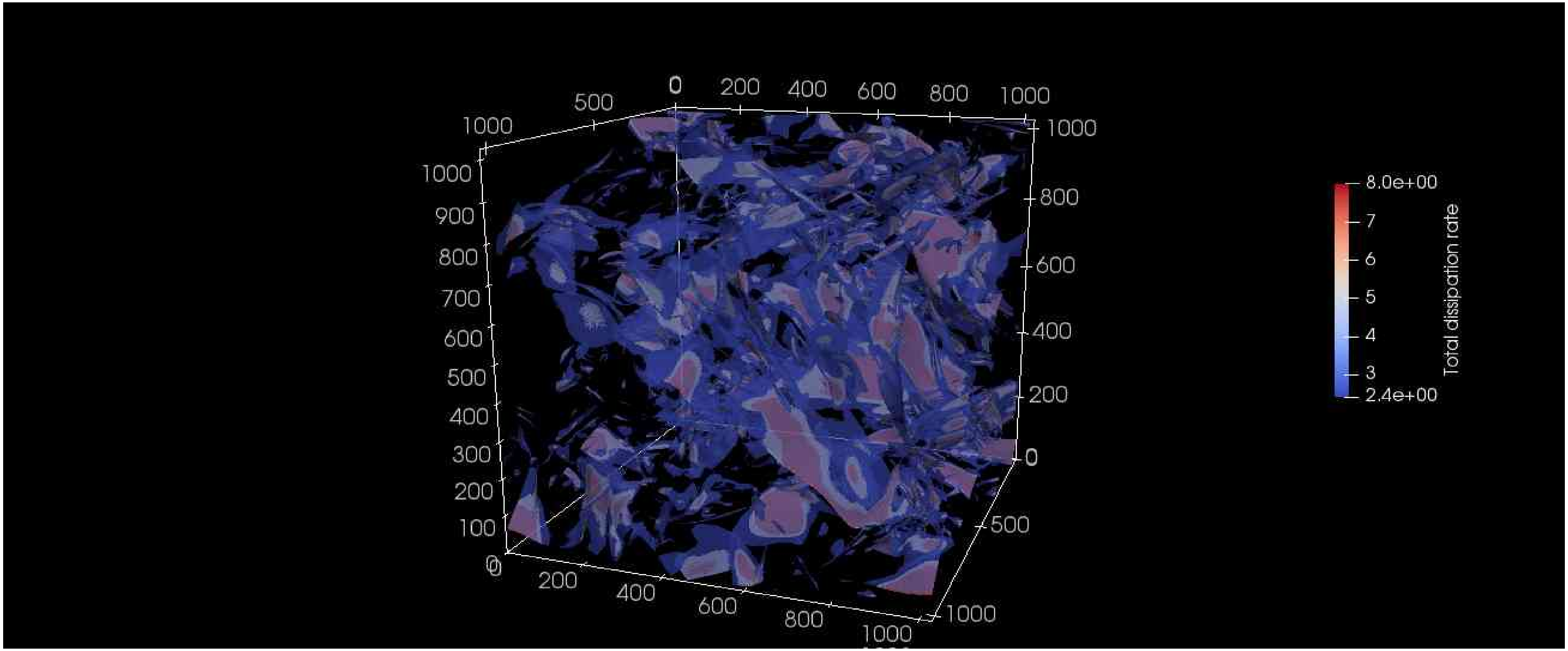

Intermittence: Less than 1% of volume, ~25% of dissipation.

Dissipative structures are organised in sheets

Numerical methods - Gradient geometry

High dissipation is correlated with strong gradients of $(\rho, \mathbf{u}, \mathbf{B}) \equiv \mathrm{W}$

➡ We design a tool to access the local geometry of gradients.

$$\partial_{\mathbf{r}} \mathbf{W} \equiv \left((\hat{\mathbf{r}} \cdot \nabla) \log \rho, \frac{1}{c} (\hat{\mathbf{r}} \cdot \nabla) \mathbf{u}, \frac{1}{c\sqrt{4\pi\rho}} (\hat{\mathbf{r}} \cdot \nabla) \mathbf{B} \right)$$

$$\widehat{\mathbf{r}} = \frac{\mathbf{r}}{|\mathbf{r}|}$$

The squared norm of this gradient :

$$||\partial_{\widehat{\mathbf{r}}} \mathbf{W}||^2 = \frac{1}{\ell_{scan}^2} \left(\widehat{\mathbf{r}} \cdot \widehat{\mathbf{r}}_{\mathrm{scan}}\right)^2 + \frac{1}{\ell_{\perp 1}^2} \left(\widehat{\mathbf{r}} \cdot \widehat{\mathbf{r}}_{\perp 1}\right)^2 + \frac{1}{\ell_{\perp 2}^2} \left(\widehat{\mathbf{r}} \cdot \widehat{\mathbf{r}}_{\perp 2}\right)^2$$

Where $\mathbf{r}_{scan}$ $\mathbf{r}_{\perp 1}$ $\mathbf{r}_{\perp 2}$ are the main axis

$$\ell_{scan} < \ell_{\perp 1} < \ell_{\perp 2}$$

→ $||\partial_{\widehat{\mathbf{r}}_{\mathbf{scan}}} \mathbf{W}||^{-1} = \ell_{scan}$

→ $||\partial_{\widehat{\mathbf{r}}_{\perp \mathbf{1}}} \mathbf{W}||^{-1} = \ell_{\perp 1}$

→ $||\partial_{\widehat{\mathbf{r}}_{\perp \mathbf{2}}} \mathbf{W}||^{-1} = \ell_{\perp 2}$

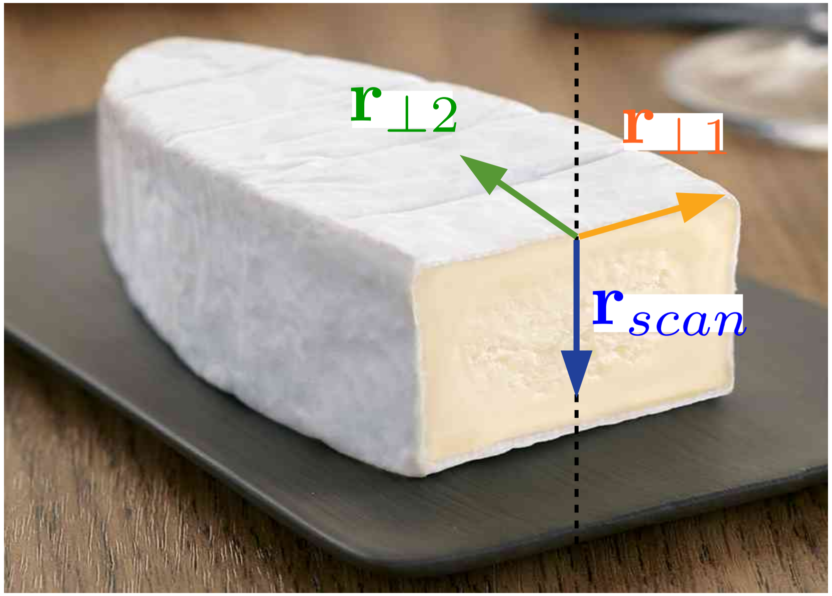

All the simulation cells

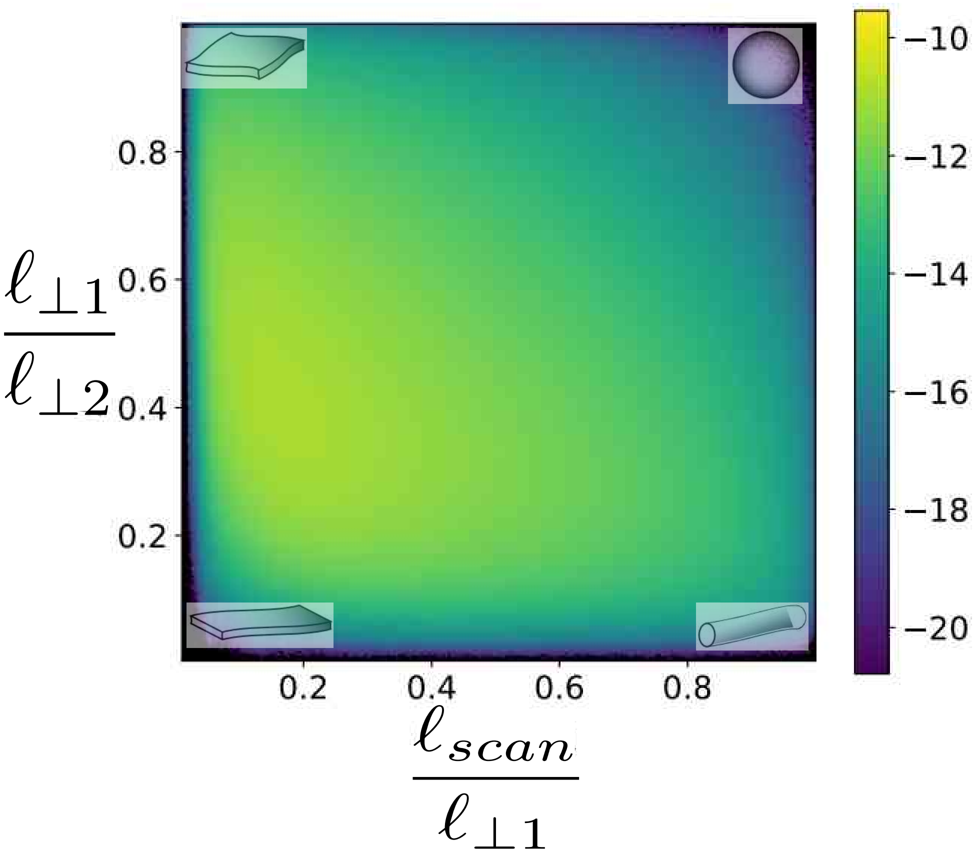

High dissipation cells

$$\epsilon \geq \langle \epsilon \rangle + 4 \times \sigma$$

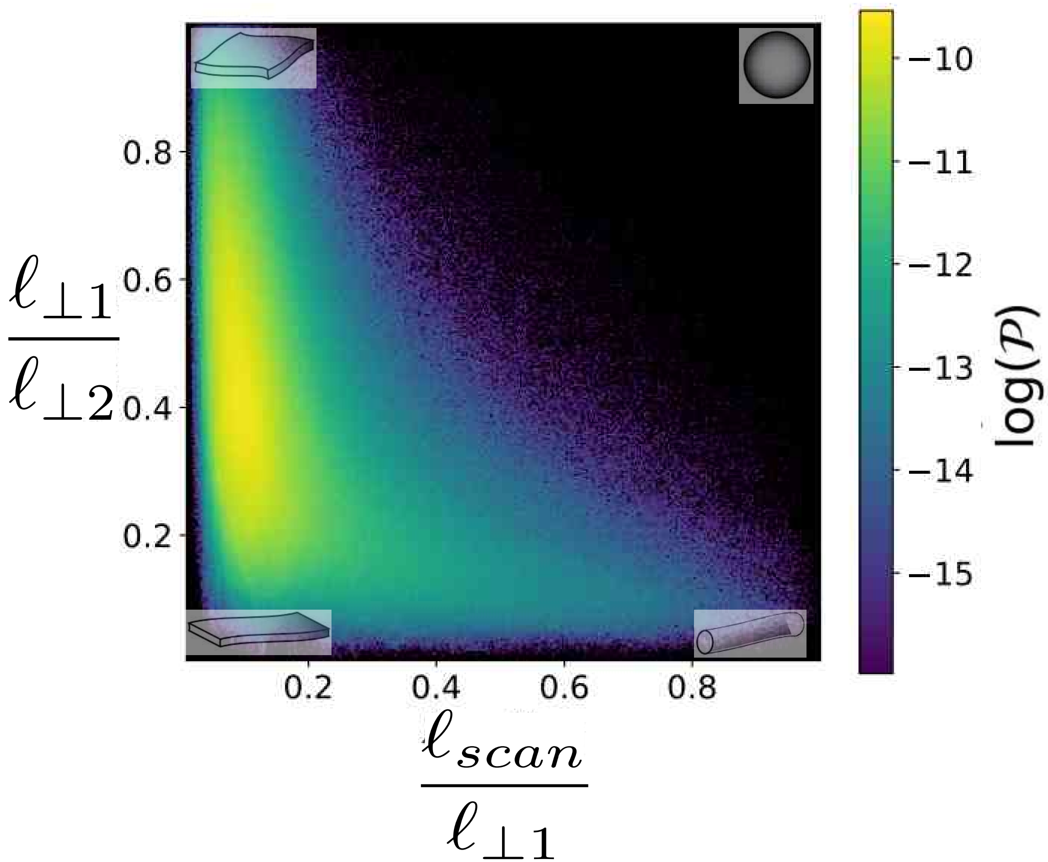

➡ Areas of high dissipation are locally planar

➡ Variations in state variables occur mainly in the direction of the scan.

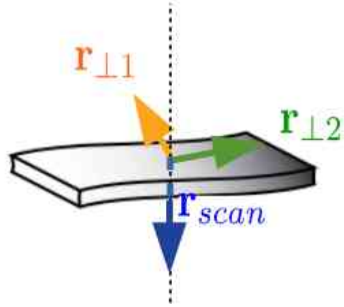

Numerical methods - Scan profiles

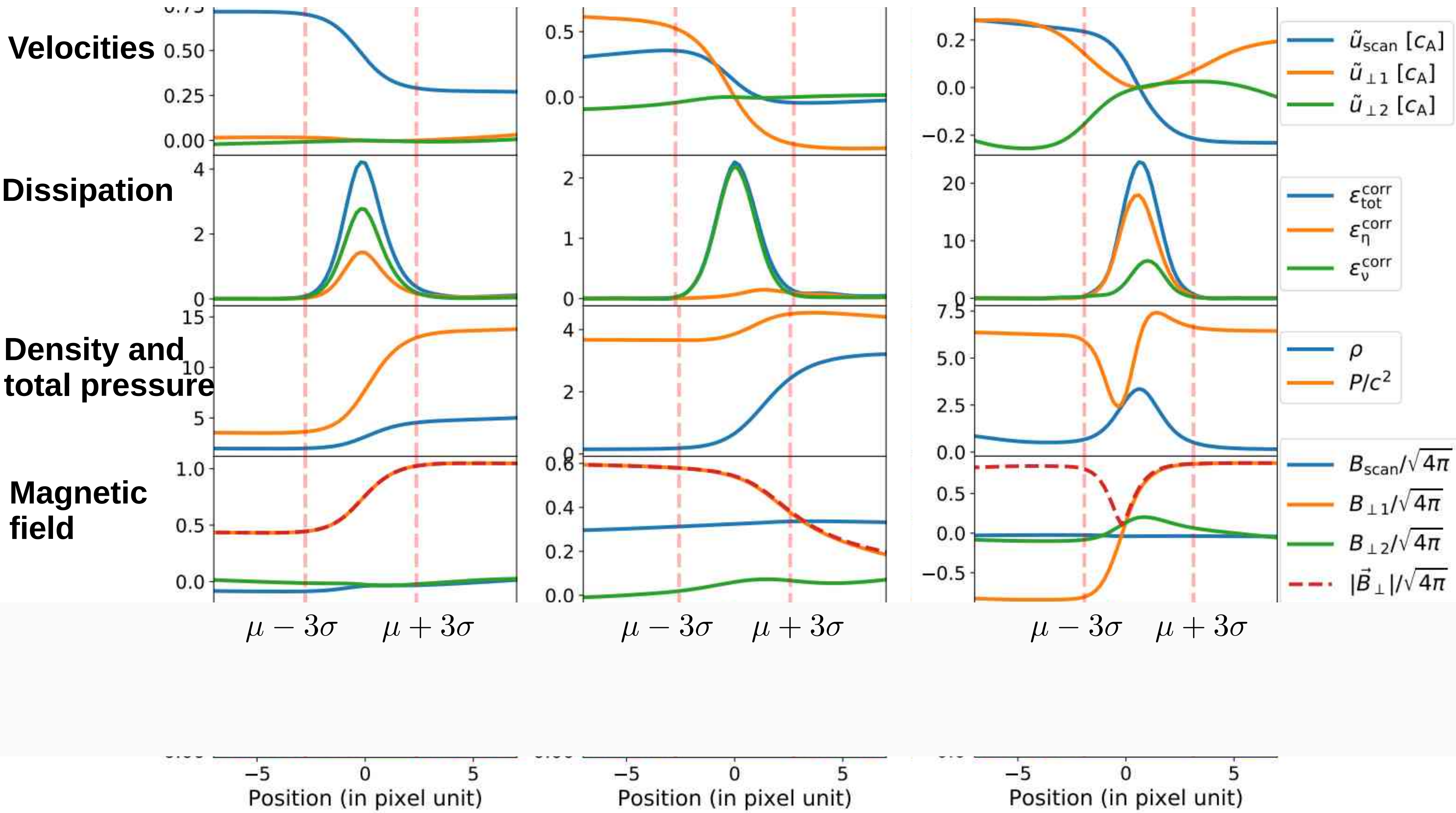

We examined a large number of profiles in order to sort them out

Fast shock | **Slow shock** | **Alfvén discontinuity**

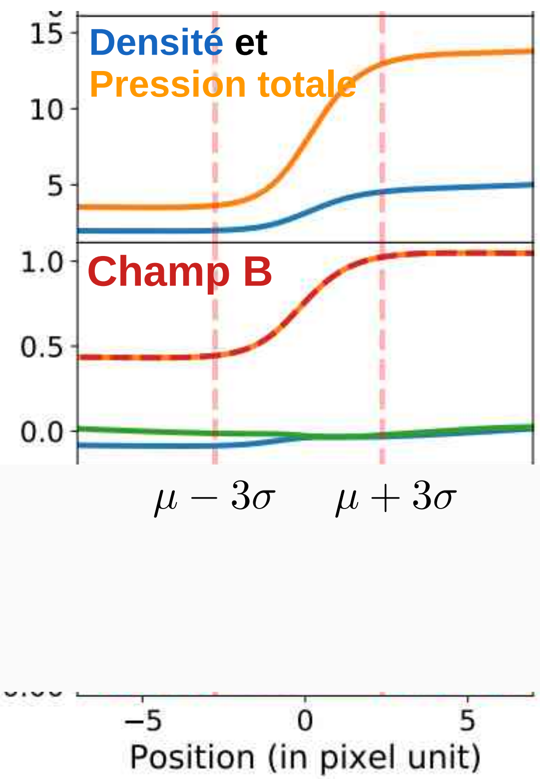

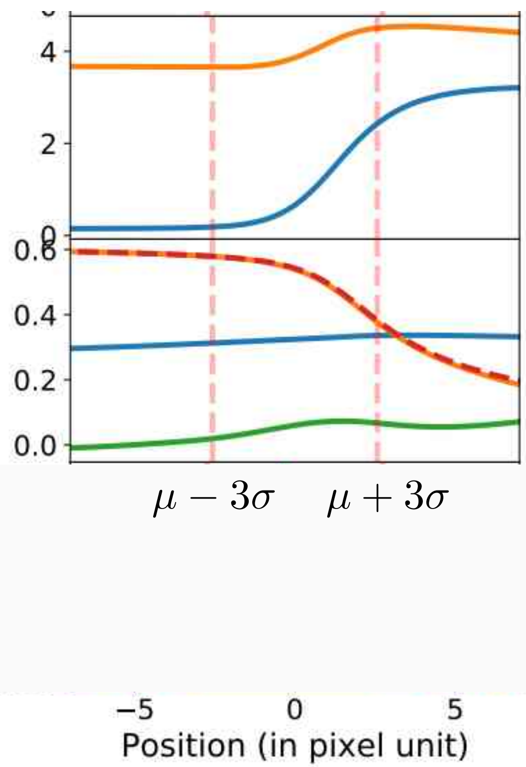

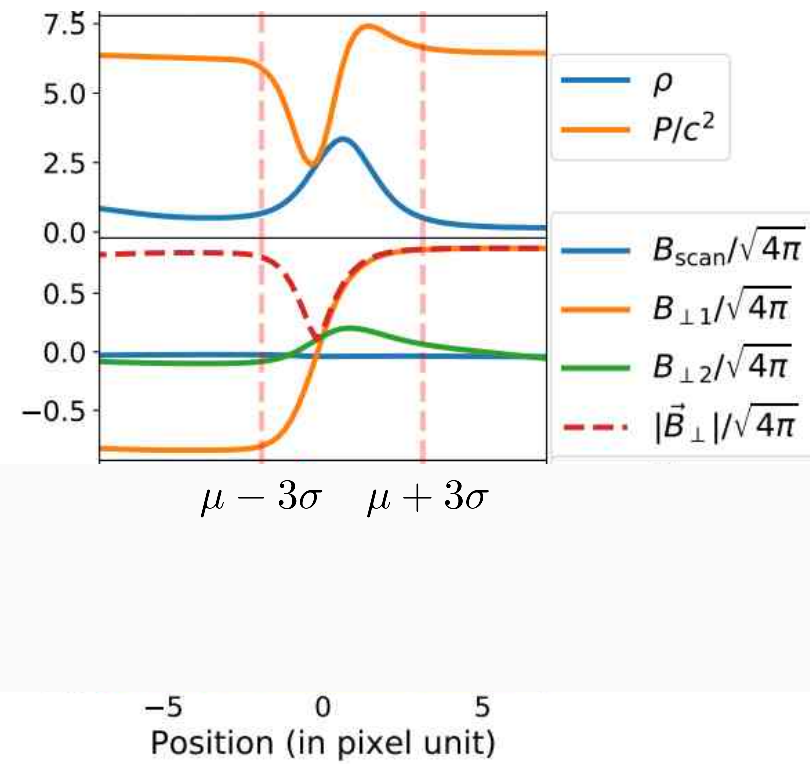

$P_{\mathrm{tot}} \nearrow \quad |\vec{B}_\perp| \nearrow$

$\rho \nearrow \quad |\vec{B}_\perp| \searrow$

$\rho \nearrow\searrow \quad |\vec{B}_\perp| \searrow\nearrow$

These are our heuristic criteria for identifying

Numerical methods - Decomposition of gradients into pure waves

In isothermal MHD there are 6 waves (3 natures x 2 directions) that can propagate when the fluid is disturbed:

Fast magnetosonic wave (right and left)
Alfvén waves (right and left)
Left magnetosonic wave (right and left)

These waves form a basis for local gradients

➡ We can always decompose the local gradients into Slow/Fast magnetosonic and intermédiaire (Alfvénique) gradients

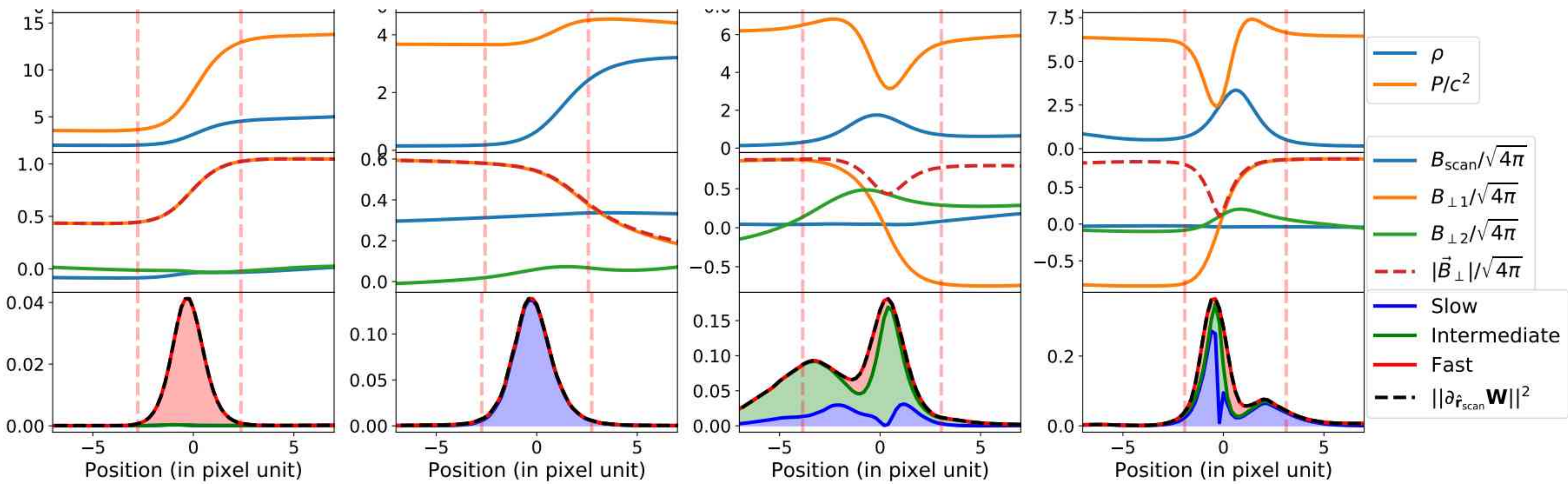

➡ **The identification is based on two independent sets of criteria (heuristic + pure wave decomposition)**

$P_{tot} \nearrow \quad |\vec{B}_\perp| \nearrow$	$\rho \nearrow \quad |\vec{B}_\perp| \searrow$	$\rho \nearrow\searrow$	$|\vec{B}_\perp| \searrow\nearrow$
Fast magnetosonique wave	Slow magnetosonique wave	Alfvén wave	Slow magnetosonique wave

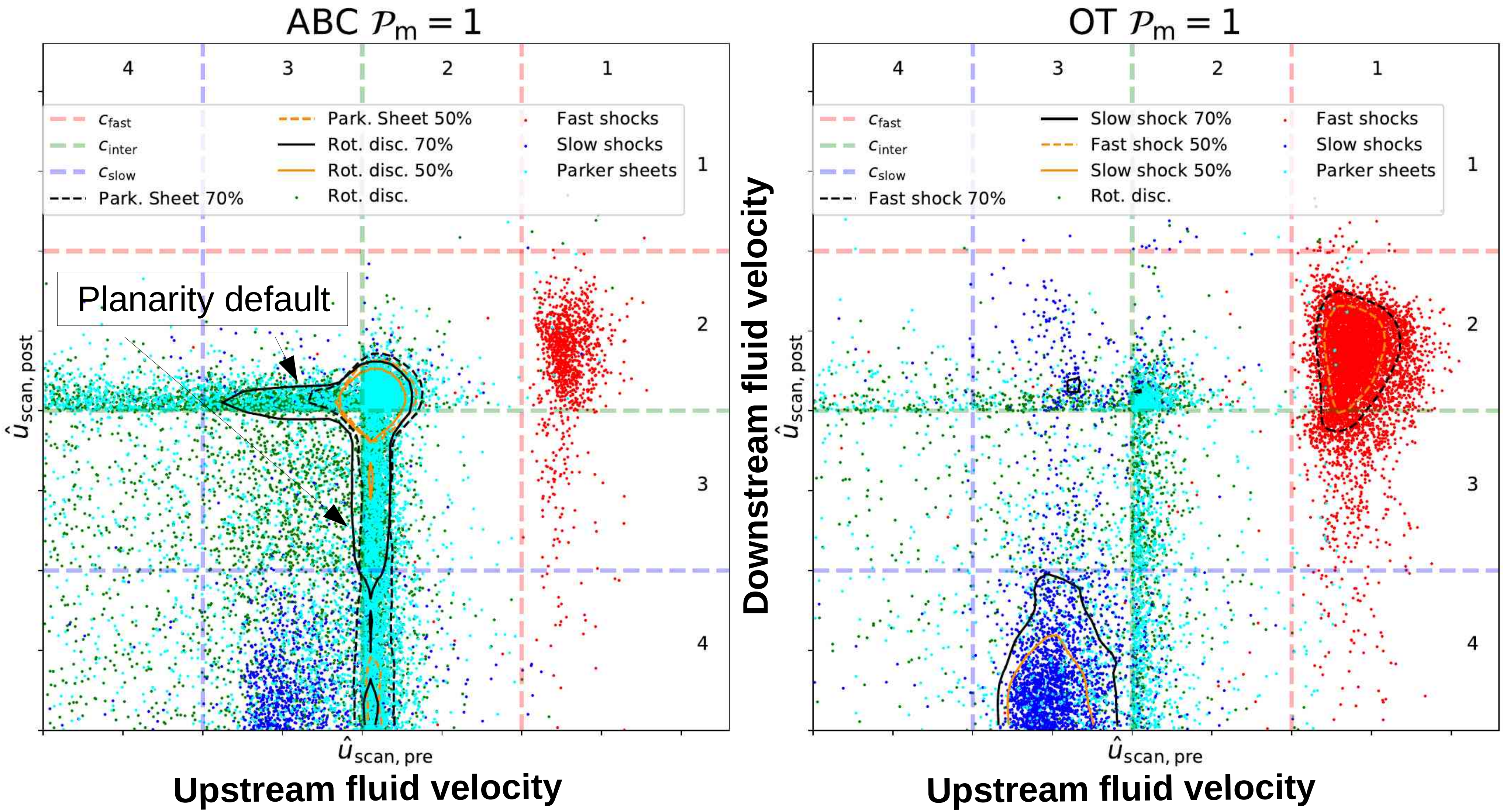

➡ The speed jumps between pre- and post-discontinuity are consistent with the identifications

Extraction and analysis of dissipative structures

We perform scans and identifications until all cells belonging to dissipation structures are identified.

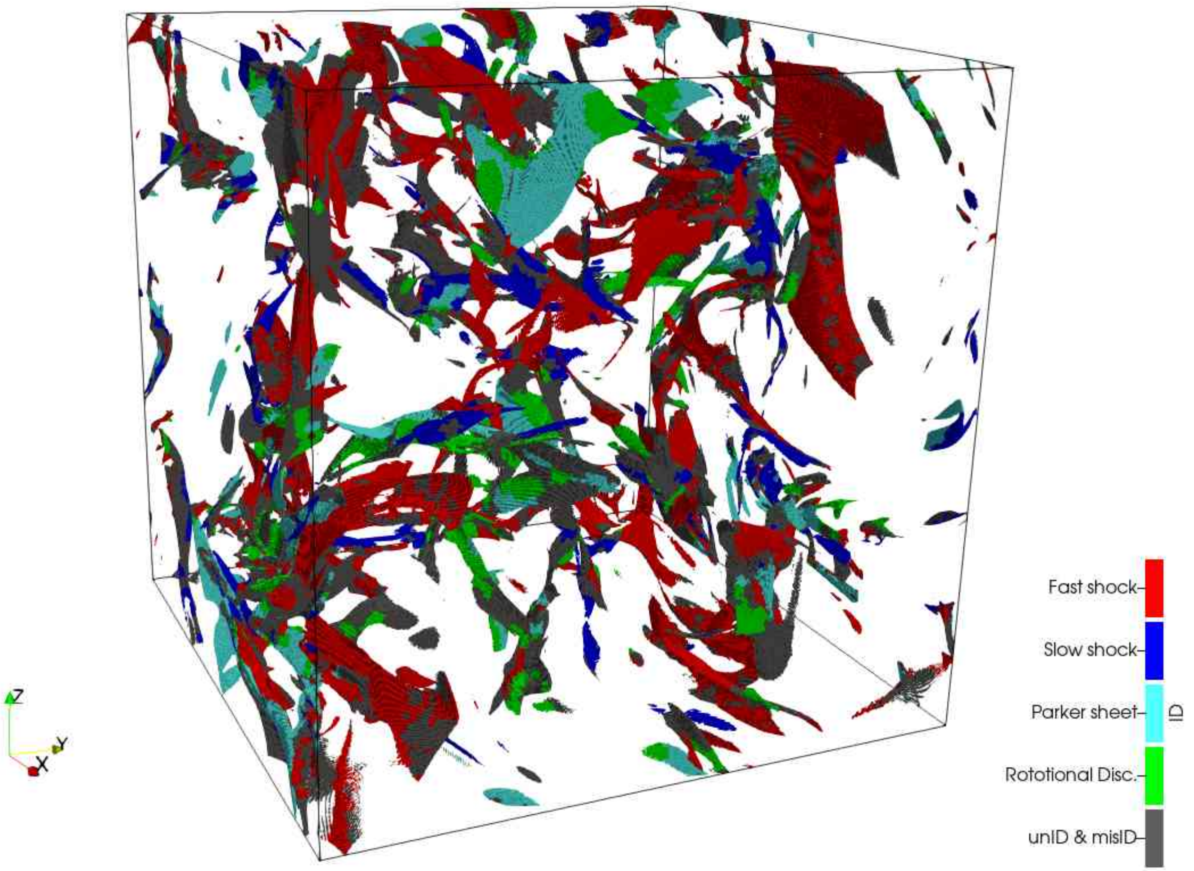

(OT near the dissipation peak)

Impact of initial conditions

OT M4 (near the dissipation peak)

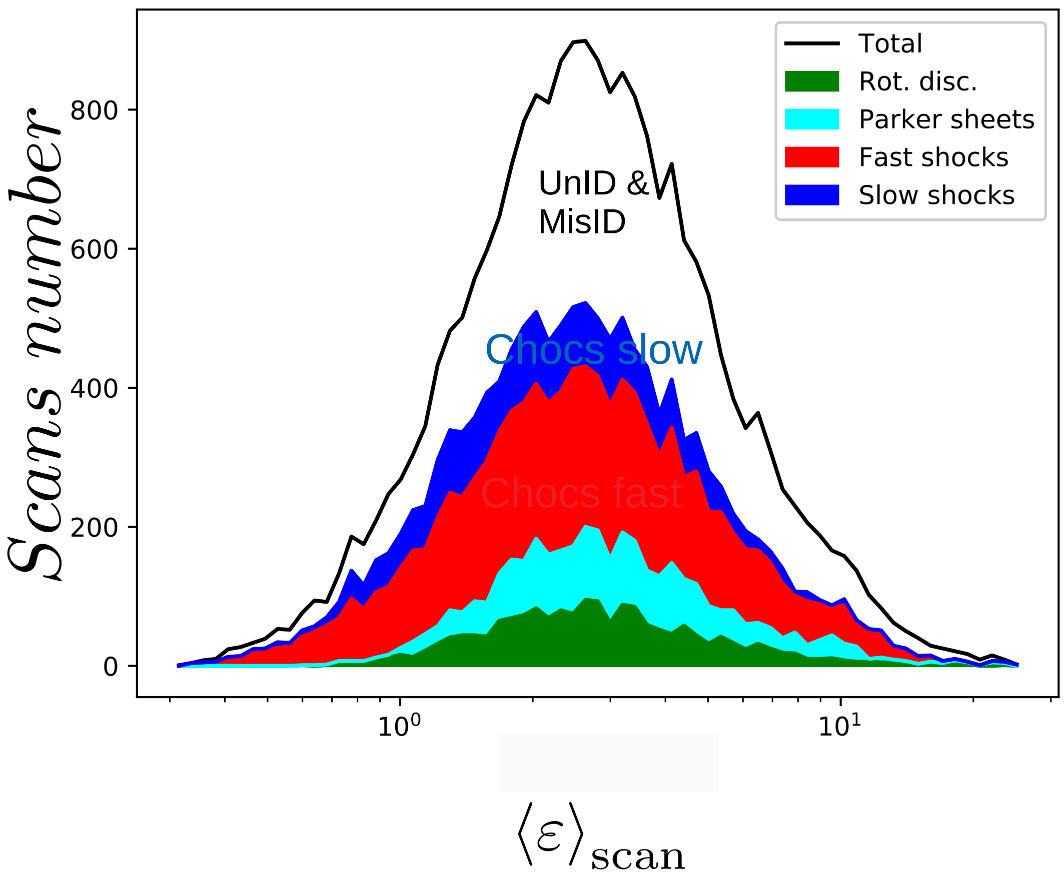

ABC M4 (near the dissipation peak)

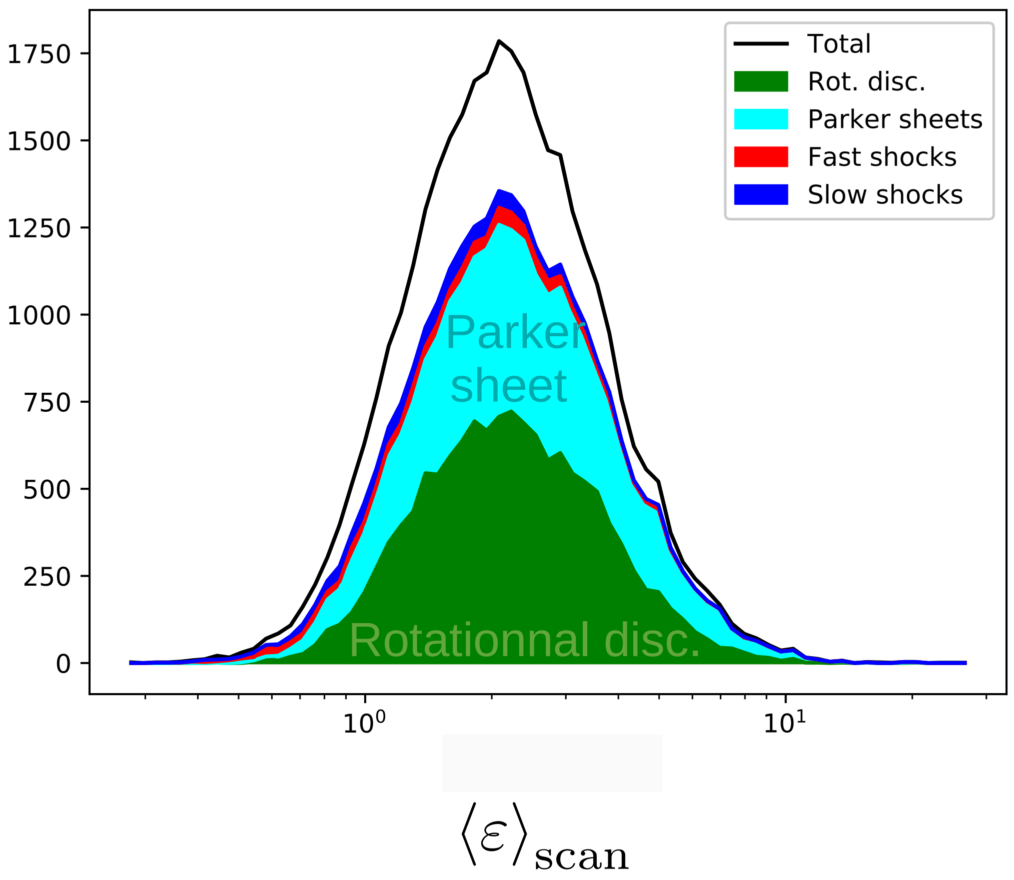

→ 59 % of scans identified

→ 74 % of scans identified

Temporal evolution of dissipation mechanisms

Comparison of initial conditions (flow) :

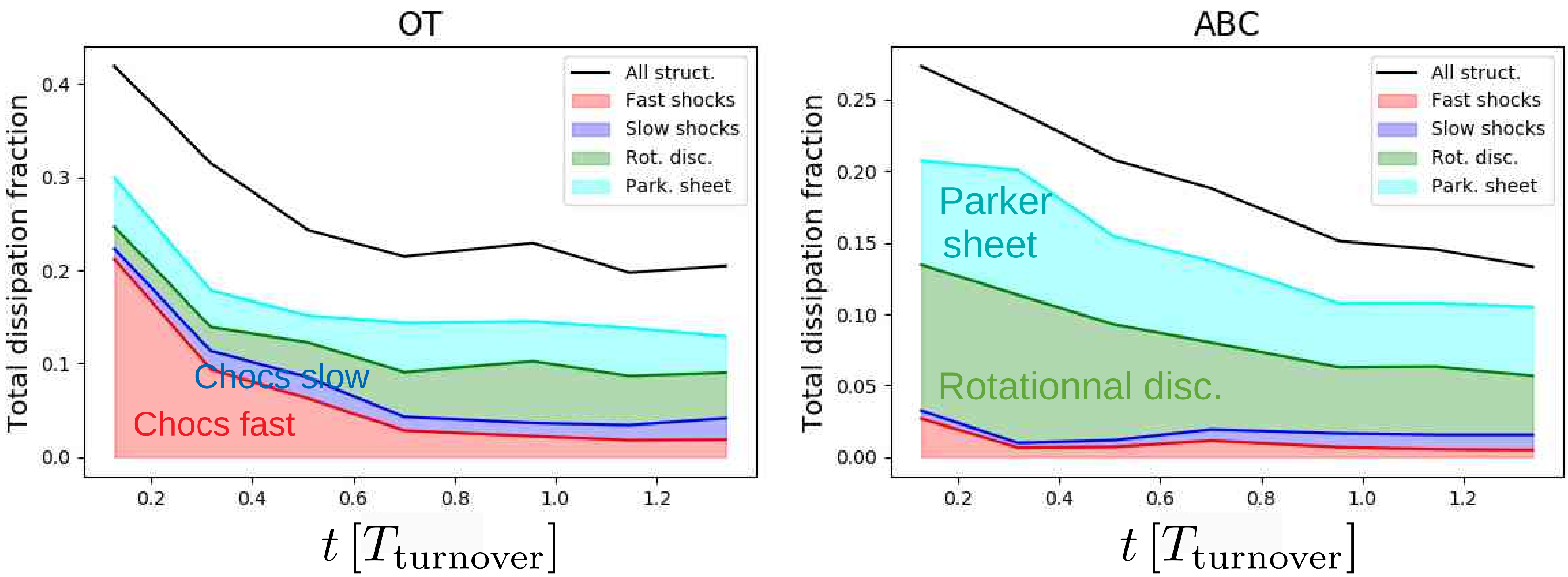

➡ The impact of the initial conditions on the structures is erased after a turnover time. Most of the dissipation then occurs in rotational discontinuities and Parker sheets

Variation of dissipative constants $\mathcal{P}m = \nu/\eta$

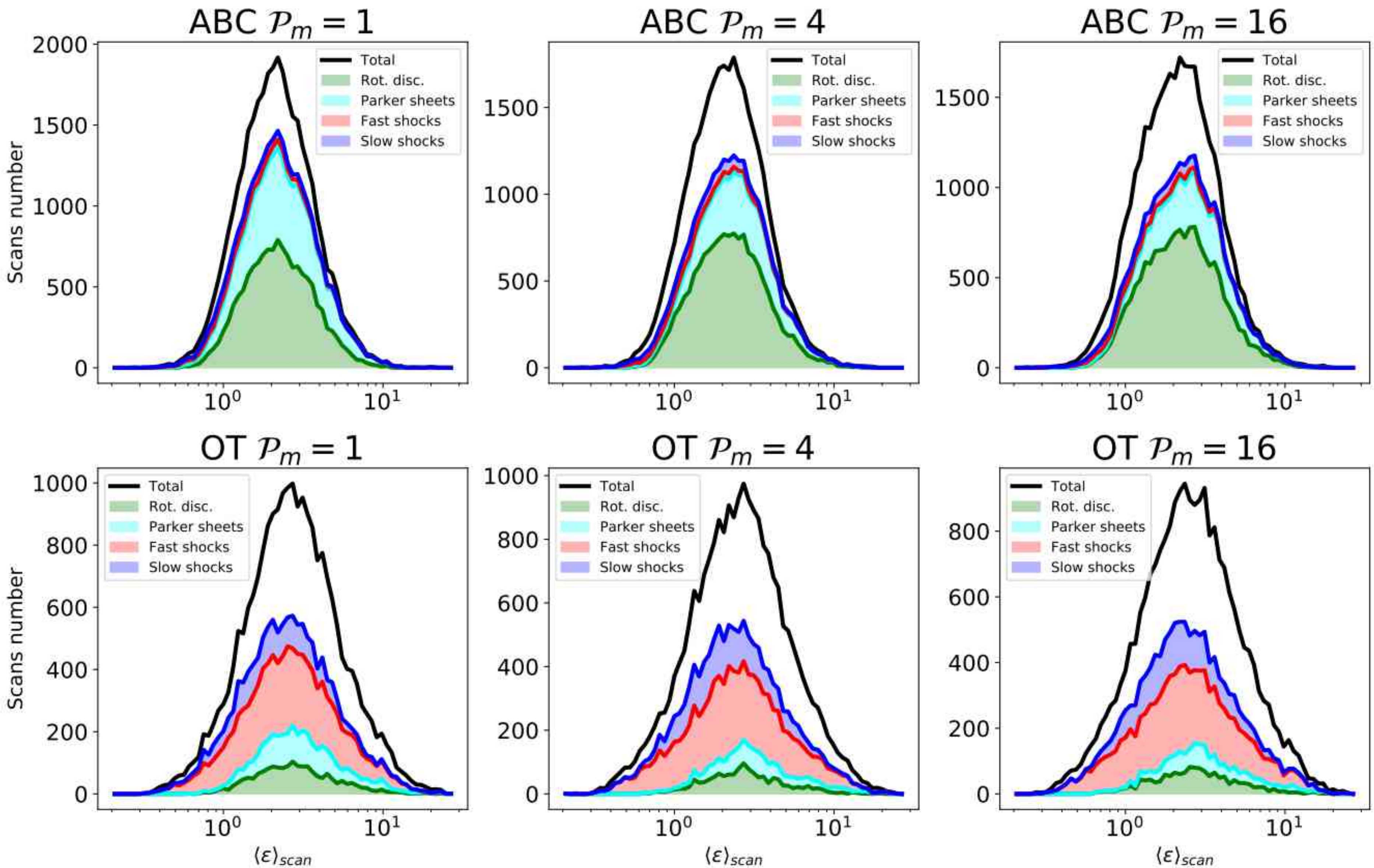

Brandenburg (2014): an increase in Pm leads to an increase in $\langle \varepsilon_\nu \rangle \;/\; \langle \varepsilon_\eta \rangle$

Variation of dissipative constants $\mathcal{P}m = \nu/\eta$

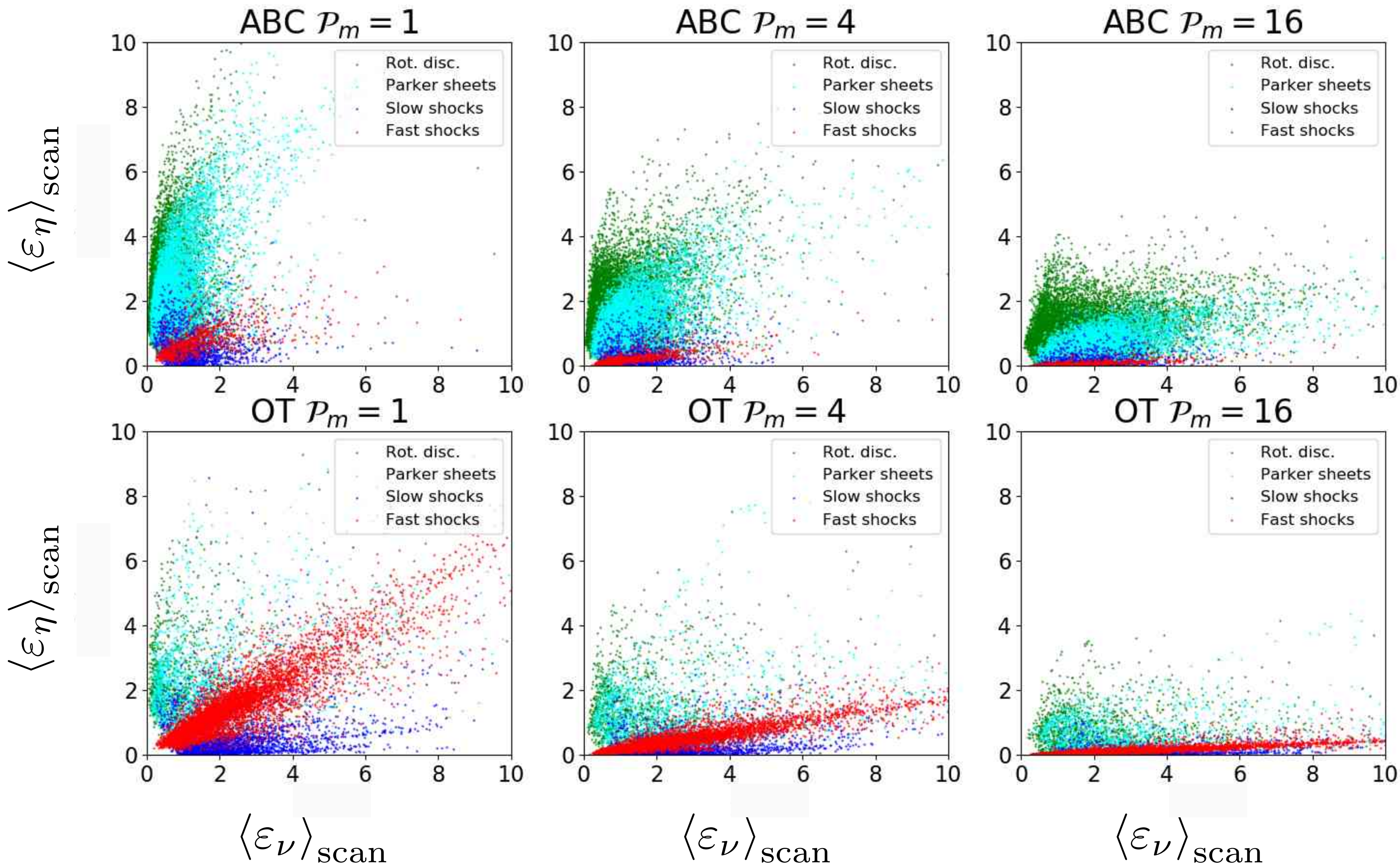

We confirm the result of Brandenburg (2014).

➡ This change is explained by the change in $\langle \varepsilon_\nu \rangle_{\rm scan} / \langle \varepsilon_\eta \rangle_{\rm scan}$

Conclusions et perspectives

What form does dissipation take in an isothermal MHD regime? In what type of structure?

- In compressible MHD turbulence, regions of high dissipation are sheets.
- Four types of dissipative structures are systematically characterized.
- Most of the dissipation occurs in rotational discontinuities and Parker sheets after a turnover time.

Numerical or physical dissipation?

- The dissipation in our simulations is a mixture of physical and numerical dissipation
  numerical dissipation (~60%-40%).
- We propose a method to recover locally the numerical dissipation.

Footprint of initial conditions ?

- The distribution of these structures depends on the initial flow at an early stage.
- The impact of the IC on these structures fades after about one turnover time.

Do the microphysical dissipative constants of the medium have an impact?

- The magnetic Prandtl number does not change the type of dissipative structures that form.
- It changes the ohmic/viscous dissipation within the dissipative layers.